Backend DC Offsets and Calibration Errors as Sources of Non-linearity

Toney Minter

May 2, 2006

1 Introduction

A radio-telescope receiver converts the incident radiation focused by the telescope onto the receiver into an analog RF signal that propagates within wires, cables, electronic components, etc. At some point this analog signal is converted into a digital signal so that it can be saved onto tape or a computer disk. The devices that convert the signal from analog to digital (A/D) will inherently have a DC offset – they will produce a non-zero digital value for a analog DC signal input. In practice we do have some control over the size of the DC offset term. It can be made small enough to be insignificant to most measurements. However, this is not always the case.

We must also correctly calibrate the resulting digitized data. If the calibration is not done correctly then we can add spurious systematic affects, such as induced non-linear responses, to the data.

Both of these issues have been factors in investigating the possible non-linear response of the GBT. In this memo we describe how calibration errors and DC offsets can lead to perceived non-linear responses for the GBT. The goal of this memo is to illustrate various areas where calibration schemes need more attention. Possible solutions are presented but are not treated rigorously with the assumption that the "Calibration Memo" presently being worked on by Ron Maddalena will handle these items rigorously.

2 Calibration Induced Non-linearities

In some of the following sections we will ignore the frequency dependence of the measurements. As such, these arguments can be taken to apply to a single frequency channel for spectral line data. However, we do note that there is usually not enough signal to noise to determine the value of the system temperature in each frequency channel so some averaging over frequencies will be necessary in practice. We will also ignore the possibility of different terms having different weighting - which could be important if using a noise diode whose equivalent temperature was nearly equal to the system temperature or for feed-arm vibration corrections to give a few examples.

2.1 Sig-Ref/Ref Measurements

Historically the standard $(Sig - Ref)/Ref$ type calibration done in the AIPS++/DISH (Nod calibration only) [1] and in GBTIDL version 1.1 and earlier packages have had an error. (This was determined by looking at the source code for each of these programs.) In the following section I describe how this erroneous calibration can lead to the apparent non-linear response. I then point out two different methods (in reality they are equivalent but take different steps) to correctly calibrate the data without any induced non-linear response.

[1] http://wiki.gb.nrao.edu/bin/view/Data/DishUsersGuideForGBT calibration section

2.1.1 Standard Method (GBTIDL v1.1 and AIPS++/DISH Nod)

Consider any measurement that has a measurement with the signal which is to be measured (sig state) and a reference measurement (ref state). Furthermore, let the noise diodes be switched on and off for both the sig and ref states. This data is typically reduced using

$$T_{src} = \frac{\left[S^{on}_{sig} + S^{off}_{sig}\right] - \left[S^{on}_{ref} + S^{off}_{ref}\right]}{\left[S^{on}_{ref} + S^{off}_{ref}\right]} \cdot T_{sys} \quad (1)$$

where

$$T_{sys} = \frac{S^{off}_{ref}}{\left[S^{on}_{ref} - S^{off}_{ref}\right]} \cdot T_{cal} \quad (2)$$

and T_{cal} is the blackbody temperature equivalent of the noise diode contribution to the signal, S are the raw count values measured by the backend, the subscript indicates where the data are from a reference or signal measurement and the superscript indicates if the noise diode was on or off. Equation 1 uses the standard practice of averaging together both the noise diode on and off states for each sig and ref measurement as the first step to reducing the data.

The contributions to S are from the astronomical source of interest, $S(src)$, from the astronomical background, the sky, the telescope and the IF system, $S(sys)$, the noise diode, $S(cal)$, and from the DC offset $S(DC)$. Substituting these into equations 1 and 2 results in:

$$T_{src} = \frac{S(src)}{[S(sys) + S(cal)/2 + S(DC)]} \cdot T_{sys} \quad (3)$$

and

$$T_{sys} = \frac{[S(sys) + S(DC)]}{S(cal)} \cdot T_{cal}. \quad (4)$$

Combining equations 3 and 4 gives us

$$T_{src} = \frac{S(src) \cdot [S(sys) + S(DC)]}{[S(sys) + S(cal)/2 + S(DC)] \cdot S(cal)} \cdot T_{cal}. \quad (5)$$

As can be seen from equation 5, if the noise diode is not fired then the DC offset term and system term are removed from the result. However, when the noise diode is fired and the on and off states of the noise diode are averaged together in the data reduction, we see that the noise diode and DC offset term combine to produce a non-linear response of the system as a whole, i.e. $T_{src} \neq \frac{S(src)}{S(cal)} \cdot T_{cal}$. This is demonstrated in Figure 1 where we have defined

$$S(nonlinear) = \frac{S(sys) + S(DC)}{S(sys) + S(cal)/2 + S(DC)}. \quad (6)$$

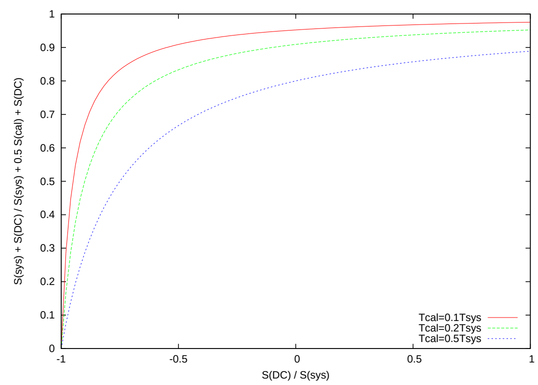

Figure 1: Plot of $S(nonlinear)$ versus $S(DC)$ for different values of $S(cal)$. Both $S(DC)$ and $S(cal)$ values are represented as fractions of the value of $S(sys)$ to allow these graphs to be applied to any telescope. If the $S(cal)$ term was not present then these values would all be one.

The DC offsets are expected to change in time. The time scale over which this happens is uncertain. It is possible that the DC offset terms could change with the ambient temperature of the backend and IF Rack. The ambient temperature changes every few minutes as the HVAC systems turn on and off. The noise diode equivalent blackbody temperatures are also known to change over year time scales for some receivers. This means that repeated observations could result in different values of the non-linear term, $S(nonlinear)$.

This erroneous calibration will also introduce baseline structure into the resulting data. It is well known that the GBT $T_{sys}(\nu)$ and $T_{cal}(\nu)$ values each have frequency structure. Furthermore these frequency structures are independent of each other. The frequency structure of $T_{sys}(\nu)$ and $T_{cal}(\nu)$ enter into the mis-calibration through non-linear term shown in equation 6. This is easily illustrated via the following example in which we consider that the DC offset term and the noise diode contributions are $\leq 0.1 \cdot T_{sys}$. This allows us to perform a Taylor expansion of equation 6. Keeping only the lowest order terms we have

$$S(nonlinear) \sim 1 - \frac{1}{2}\frac{S(cal)}{S(sys)} \tag{7}$$

which means that some frequency structure of the order of $0.5S(cal)/S(sys)$ will be introduced into the spectrum - even if only a scalar value of $S(cal)$ is used for the calibration.

It should be noted that these errors have been corrected in GBTIDL version 1.2 and later.

2.1.2 Alternative Method 1

Now let us consider an alternative to the above data reduction. In this alternative method we will reduce each noise diode state independently and then average the results together. This results in

$$\begin{aligned}
T_{src}^{on} &= \frac{S_{sig}^{on} - S_{ref}^{on}}{S_{ref}^{on}} \cdot T_{sys}^{on} && (8)\\
&= \frac{S(src)}{S(sys) + S(cal) + S(DC)} \cdot T_{sys}^{on} && (9)\\
T_{src}^{off} &= \frac{S_{sig}^{off} - S_{ref}^{off}}{S_{ref}^{off}} \cdot T_{sys}^{off} && (10)\\
&= \frac{S(src)}{S(sys) + S(DC)} \cdot T_{sys}^{off} && (11)
\end{aligned}$$

with

$$\begin{aligned}
T_{sys}^{on} &= \frac{S_{ref}^{on}}{\left[S_{ref}^{on} - S_{ref}^{off}\right]} \cdot T_{cal} && (12)\\
&= \frac{[S(sys) + S(cal) + S(DC)]}{S(cal)} \cdot T_{cal} && (13)\\
T_{sys}^{off} &= \frac{S_{ref}^{off}}{\left[S_{ref}^{on} - S_{ref}^{off}\right]} \cdot T_{cal} && (14)\\
&= \frac{[S(sys) + S(DC)]}{S(cal)} \cdot T_{cal} && (15)
\end{aligned}$$

and subsequently combining equations 8 through 15 gives

$$\begin{aligned}
T_{src}^{on} &= \frac{S(src)}{S(cal)} \cdot T_{cal} && (16)\\
T_{src}^{off} &= \frac{S(src)}{S(cal)} \cdot T_{cal} && (17)\\
T_{src} &= \frac{T_{src}^{on} + T_{src}^{off}}{2} && (18)\\
&= \frac{S(src)}{S(cal)} \cdot T_{cal} && (19)
\end{aligned}$$

which as we can see does not have any non-linear response.

2.1.3 Alternative Method 2

Another way to correct for the DC offset and T_{cal} induced non-linearity is to replace T_{sys} with

$$\begin{aligned}
T'_{sys} &= \left[T_{sys}^{on} + T_{sys}^{off}\right]/2 && (20)\\
&= \frac{[S(sys) + S(cal)/2 + S(DC)]}{S(cal)} \cdot T_{cal} && (21)
\end{aligned}$$

in equation 1 which then removes the non-linearity in equation 5. Combining equations 21 and 3 results in

$$T_{src} = \frac{S(src)}{S(cal)} \cdot T_{cal} \tag{22}$$

which is equivalent to the result found in Method 1.

This second method is what is implemented in GBTIDL beginning with a patch to version 1.2.

2.2 Total Power Measurements

In total power continuum measurements the noise diode is turned on and off while the telescope takes data. This can be either while sitting at a specific location or while the telescope is moving (i.e. mapping).

2.2.1 "Standard AIPS++ Continuum" Method

In the standard AIPS++ continuum data reduction, pairs of noise diode on and off data are used from within a single integration. For the ith integration the calibration becomes

$$T^i_{src} = \frac{\left[S^i_{on} + S^i_{off}\right]}{2} \cdot G^i_{sys} \tag{23}$$

$$G^i_{sys} = \frac{T_{cal}}{\left[S^i_{on} - S^i_{off}\right]}. \tag{24}$$

Now we can assume that $S(sys)$ and $S(DC)$ are constant during the time that the noise diode is turned on and off. However, we can't make this assumption about $S(src)$ since the telescope may be mapping across a continuum source, etc. So we have to use a different $S(src)$ for when the noise diode is on and off. Letting

$$S^i_{on}(src) = S^i_{off}(src) + \Delta S^i(src) \tag{25}$$

we obtain

$$G^i_{sys} = \frac{T_{cal}}{[\Delta S^i(src) + S(cal)]} \tag{26}$$

$$\begin{aligned} T^i_{src} &= \left\{S^i_{off}(src) + \Delta S^i(src)/2 + S(cal)/2 \right. \\ &\quad \left. + S(sys) + S(DC)\right\} \cdot G^i_{sys} \qquad (27) \\ &= \left(\frac{S^i_{off}(src) + S(sys) + S(DC)}{\Delta S^i(src) + S(cal)} \right. \\ &\quad \left. + \frac{1}{2}\right) T_{cal} \qquad (28) \end{aligned}$$

which is significantly different than the desired

$$T^i_{src} = \left(\frac{\left[S^i_{off}(src) + S(sys)\right]}{S(cal)} + \frac{1}{2}\right) T_{cal} \tag{29}$$

because of the contributions of the DC offset term and due to changes in the source contribution during the time it takes to turn on and off the noise diode.

If the switching period (i.e the time to do a cycle of the noise diode on and off) is small relative to the time it takes $S(src)$ to change as the telescope moves across the sky, then we can assume that to first order that

$$\Delta S^i(src) \sim \frac{\partial S(Src)(\alpha, \delta)}{\partial X(\alpha, \delta)} \tag{30}$$

where $X(\alpha, \delta)$ is the vector that the telescope motion takes across the sky. For a point source, we would expect $S(src)$ (the telescopes response to the source) to be a Gaussian and $\Delta S^i(src)$ would take the form shown in Figure 2. This is indeed what is observed as we can see from a continuum observation that scanned across the Galactic Plane and several point-like sources which is presented in Figure 3. Figure 3 shows the values of $\Delta S^i(Src)+S(cal)$ used in the gain determination. The results of calibrating this data using equation 28 are shown in Figure 4. You can easily see negative dips on either side of point-like sources which have been artificially created by the calibration scheme used.

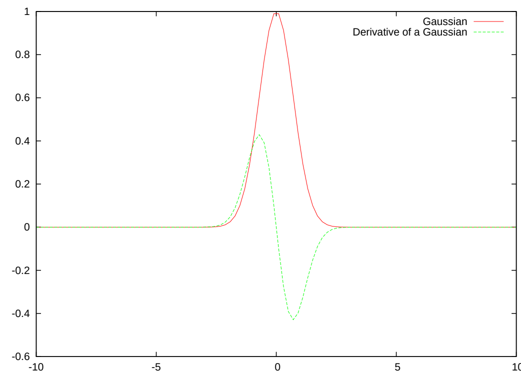

Figure 2: The expected shape of $S(src)$ for a point source – a Gaussian, and of $\Delta S(src)$ – the derivative of a Gaussian.

2.2.2 An Improved Method

We can improve the calibration by replacing the gain determined in equation 24 with

$$G^i_{sys} = \frac{T_{cal}}{\left\langle S^i_{on} - S^i_{off}\right\rangle_N} \tag{31}$$

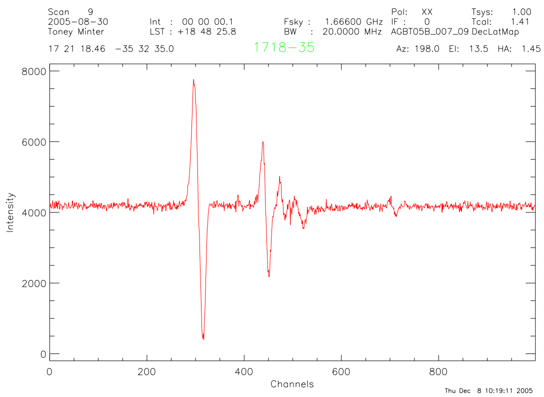

Figure 3: A plot of $\Delta S^i(Src) + S(cal)$ from a scan with the GBT across the Galactic Plane and several point-like sources.

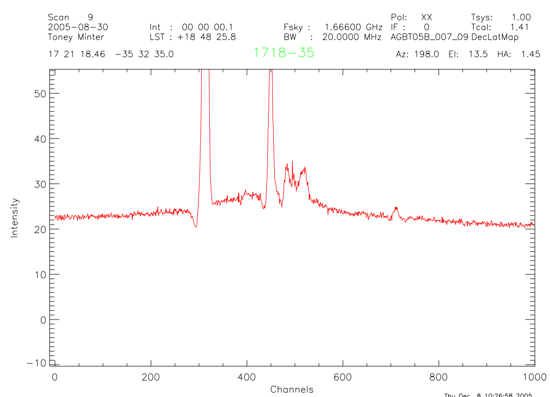

Figure 4: A plot of the calibrated (using equation 28 for the data also shown in Figure 3. Notice the artificially created negative digs on either side of a point-like source.

where $\langle ... \rangle_N$ indicates an average over N pairs of noise diode on and off data. This then gives

$$G^i_{sys} = \frac{T_{cal}}{\left\langle S^i_{on}(src) - S^i_{off}(src) + S(cal) \right\rangle_N} \quad (32)$$

$$= \frac{T_{cal}}{\langle S^i_{on}(src)\rangle_N - \left\langle S^i_{off}(src)\right\rangle_N + \langle S(cal)\rangle_N} \quad (33)$$

$$G^i_{sys} = \frac{T_{cal}}{\langle S(cal)\rangle_N} \quad (34)$$

if the telescope is moved slow enough so that $\left\langle S^i_{on}(src)\right\rangle \sim \left\langle S^i_{off}(src)\right\rangle$ and given that the source contribution and the noise diode contribution are not correlated. The final calibrated signal is then

$$T^i_{src} = \left(\frac{S^i_{off}(src) + \Delta S^i(src)/2 + S(sys) + S(DC)}{\langle S(cal)\rangle_N} + \frac{1}{2} \right) \cdot Tcal. \quad (35)$$

Now we must ask how large should N be so that the error in determining the gain does not strongly affect the error in determining T_{src}? A rough estimate is

$$N \geq \left[\frac{T_{sys} + T_{src} + ...}{T_{cal}} \right]^2 \quad (36)$$

(the reader is referred to the "Calibration Memo" currently under preparation by R. Maddalena for the precise derivation). When using a noise diode such that $T_{cal} \sim T_{sys}$ then N can be of the order of a few samples. When using a noise diode such that $T_{cal} \sim 0.1 \cdot T_{sys}$ then N needs to be of the order of hundreds.

In Figure 5 we show the gain determined from equation 31 compared with that determined from equation 24. It is easily seen that the gain from equation 31 is a much more reasonable value to use. In Figure 6 we compare the calibrated data using equation 18 with that using equation 28. As can be seen, the improved calibration has a larger signal-to-noise, does not have negative features around the point-like sources and gets the flux of the point-like sources correct.

In using equation 18 to calibrate the data, it is possible to determine the contribution from $S(sys)$ and $S(DC)$ by observing blank sky where no emission is expected. If there is emission at every point on the sky that you would like to measure then another

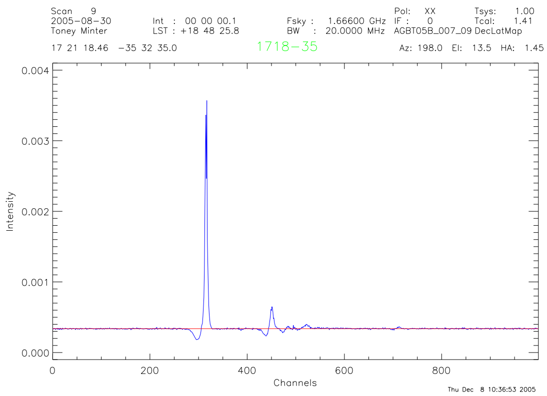

Figure 5: A plot of the gain from equation 31. The blue line is the badly calculated gain and the red line is the improved calculation of the gain.

means of determining $S(sys)$ and $S(DC)$ would have to be used such as using hot/cold loads in front of the receiver. The observer also needs to remember to remove the value of $\frac{1}{2}T_{cal}$ in this case also.

2.3 Antenna Servo System and Feed-arm Vibration Induced Calibration Errors

The GBT antenna servo system maintains the GBT position to within about 3 arc-seconds standard deviation. A plot of these deviations is shown in Figure 7. There are two important things to note from Figure 7: 1) The antenna typically takes about 5-10 seconds to get "on-source" after a scan starts; and 2) the errors in the GBT servo system are not randomly distributed.

That the antenna is not on source for the first 5-10 seconds of a scan means that we must always flag any data whose integration lies within the period of when the antenna is not yet on source.

The shape of the servo system errors can essentially be ignored. This is because the telescope's beam is Gaussian in shape (at least above the half power points) so that the same radius error from the

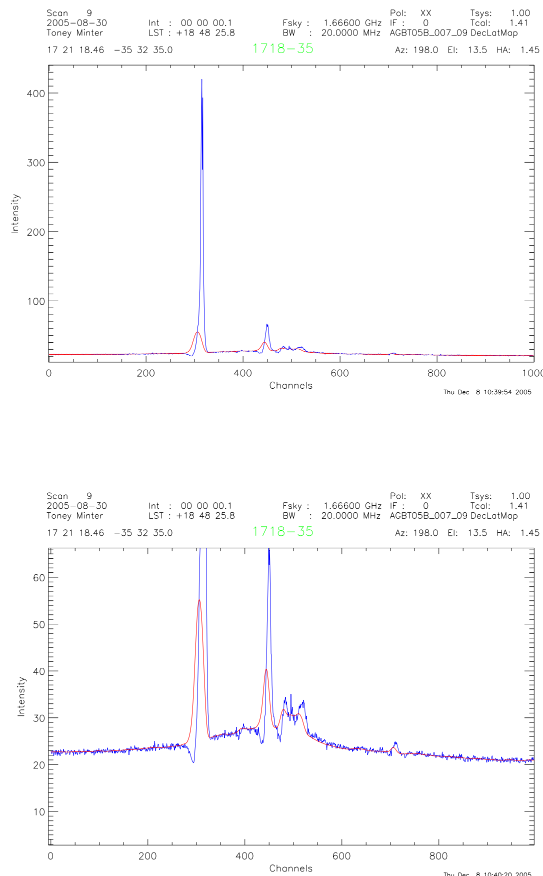

Figure 6: A plot of the calibrated data from equation 18. The top figure shows the entire range while the bottom figure shows a zoom in on the baseline. The badly calibrated data are shown in blue and the corrected calibrated data are shown in red. Note that the bad calibration gets the source fluxes incorrect and that the noise is also higher in that data since the number of points contributing to a gain value are fewer.

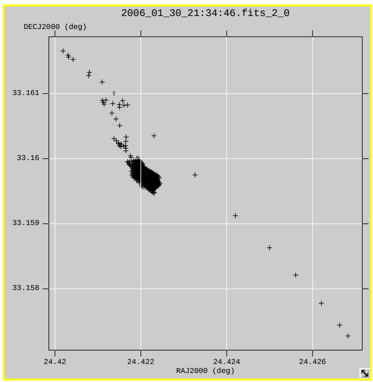

Figure 7: A plot of the GBT positions in RA and Dec sampled every 0.1 seconds while the telescope was commanded to track a single position for two minutes.

commanded position will always produce the same gain response of the telescope no matter the position angle of the servo error. Taking $\sigma_{ant}(t)$ be the antenna servo system error, at time t, in the radial direction away from the commanded position and with Ω_{ant} being the FWHM beam size of the antenna, we can set the gain of the telescope to be

$$G_{ant}(t) = G_{ant}^{max}\left\{1 - \exp\left(-4\ln 2\left[\frac{\sigma_{ant}(t)}{\Omega_{ant}}\right]^2\right)\right\} \quad (37)$$

where G_{ant}^{max} is the gain expected if we have a perfectly pointed telescope. So we need to correct for the measured source flux such that

$$S(src)(t) \rightarrow S(src)(t) \cdot \left\{1 - \exp\left(-4\ln 2\left[\frac{\sigma_{ant}(t)}{\Omega_{ant}}\right]^2\right)\right\} \quad (38)$$

for point sources. For resolved sources we will have to know the direction of the servo system error and use *a priori* knowledge of the source structure to correct the data which is beyond the scope of this memo.

Finally, for blank sky we can assume that the sky is contributing the same flux no matter what the servo error may be.

Assuming that we can replace the servo error at time t with the standard deviation of the servo errors when averaged over a whole scan, then equation 35 becomes

$$T_{src} = \frac{S(src)}{S(cal)} \cdot T_{cal} \cdot \left\{1 - \exp\left(-4\ln 2\left[\frac{\sigma_{ant}}{\Omega_{ant}}\right]^2\right)\right\}. \quad (39)$$

The slewing of the telescope to a new position, the wind, etc. can induce feed-arm vibrations in the GBT. The feed arm motions also cause the telescope beam to move around on the sky. This means that we can just replace σ_{ant} with

$$\sigma_{ant}(t) = \sqrt{\sigma_{servo}^2(t) + \sigma_{feed-arm}^2(t)} \quad (40)$$

to include the feed-arm vibrations with the above mentioned servo system errors. However, unless continuously driven, the feed-arm vibrations will damp with time. This means that the servo system and feed-arm vibration induced pointing errors must be taken out on an integration by integration basis.

2.4 Determining T_{cal} from Astronomical Measurements

The best way to determine the values of T_{cal} with 1 MHz or better resolution is to make astronomical observations of sources with known brightness temperatures. These observations would sit on the peak of the source flux and turn the noise diodes on and off until the necessary signal to noise is reached.

Under these circumstances the only contribution to $\Delta S(src)$ will be from the antenna servo system (ignoring feed-arm vibrations). Since the telescope is nominally pointed at the peak of the source flux, the servo system will always make $\Delta S(src) < 0$. Letting σ_{ant} be the standard deviation of the antenna servo system and with Ω_{ant} being the beam size of the antenna, we can set

$$\langle S(src) + \Delta S(src)\rangle_N = \left\langle S^i(src)\right\rangle_N \cdot \left\{1 - \exp\left(-4\ln 2\left[\frac{\sigma_{ant}}{\Omega_{ant}}\right]^2\right)\right\} \quad (41)$$

where we have averaged over N noise diode on/off cycles. Here N must be large enough not only to not add significantly to the noise in the calibration but must also be large enough that the standard deviation of the servo system pointing errors is sufficiently measured.

In order to determine T_{cal}, measurements of the antenna servo standard deviation, the system temperature from blank sky observations and the DC offsets must be made. The system temperature and the DC offset contributions can be removed by observing blank sky before and/or after the observation on the astronomical calibrator. Measurements before and after the astronomical calibrator will allow any systematic change of these terms with time to be estimated. The value of T_{cal} is determined from

$$T_{cal} = 2\ T_{src} \left[\frac{S^{on}_{ref} - S^{off}_{ref}}{S^{o}_{sig}n + S^{off}_{sig} - S^{on}_{ref} - S^{off}_{ref}} \right] \tag{42}$$

where T_{src} is known *a priori*. Using equations 41 and 42 while averaging over N noise diode on/off cycles results in

$$T_{cal} = 2\ T_{src} \left[\frac{\langle S^{i}_{cal} \rangle_N}{\langle S(src) + \Delta S(src) \rangle_N} \right]. \tag{43}$$

Assuming that the antenna servo system induced flux errors are small, equation 43 can be Taylor expanded to be

$$T_{cal} = 2\ T_{src} \left[\frac{\langle S^{i}_{cal} \rangle_N}{\langle S^{i}(src) \rangle_N} \right] \cdot \left\{ 1 + \exp\left(-4 \ln 2 \left[\frac{\sigma_{ant}}{\Omega_{ant}} \right]^2 \right) \right\} \tag{44}$$

which shows us that astronomically measured T_{cal} values can be over-estimated under observing conditions, such as windy days, when σ_{ant} is large relative to the beam size.

2.5 Mis-Calibration and the Lining Up Of Multiple Window Spectra

We now consider the calibration of spectral line data. Currently a single value of T_{sys} and T_{cal} are assumed to be valid across an entire spectrum. Typically average values are used. However, for the GBT and its resulting large bandwidths, this assumption is not valid and can lead to some major errors.

2.5.1 Standard Method (GBTIDL v1.2)

The current calibration of spectral line data uses the average over frequency when determining T_{sys} such that

$$T_{src}(\nu) = \frac{S^{on}_{sig}(\nu) + S^{off}_{sig}(\nu) - S^{on}_{ref}(\nu) + S^{off}_{ref}(\nu)}{S^{on}_{ref}(\nu) + S^{off}_{ref}(\nu)} \left\langle T_{sys} \right\rangle_\nu \tag{45}$$

where

$$\left\langle T_{sys} \right\rangle_\nu = \left\langle \frac{S^{on}_{ref}(\nu) + S^{off}_{ref}(\nu)}{S^{on}_{ref}(\nu) - S^{off}_{ref}(\nu)} \right\rangle_\nu \frac{\left\langle T_{cal}(\nu) \right\rangle_\nu}{2} \tag{46}$$

and $\langle ... \rangle_\nu$ indicates an average over frequency. This assumption is valid when the $T_{cal}(\nu)$ values and the $T_{sys}(\nu)$ values are nearly constant over the bandwidth being observed.

However, this is generally not the case for the GBT. There is significant structure in the $T_{cal}(\nu)$ values. In Figure 8 we plot the $T_{cal}(\nu)$ values for the Prime Focus 800 MHz receiver for the linear XX polarization. It is easily seen that using $\langle T_{cal}(\nu) \rangle_\nu$ could lead to errors of the order of 25% in the value of T_{cal} that should have been used.

Furthermore, at the lower frequencies where the Galactic background emission can be important, the value of T_{sys} can have a strong frequency dependence. This is illustrated in Figure 9.

2.5.2 Frequency Dependant Calibration

In order to test how bad the assumption of a constant T_{sys} and T_{cal} are, I reduced an OnOff observation of 3C 48 taken across the GBT Prime Focus 800 MHz receiver. Two 200 MHz bandwidth spectra were obtained with center frequencies of 780 and 820 MHz such that the entire nominal bandwidth of the receiver is covered. The data for each signal/reference state was flagged for major RFI contribution and then was smoothed to approximately 1 MHz resolution. This is the same resolution as the T_{cal} values available from the work of Ron Maddalena which

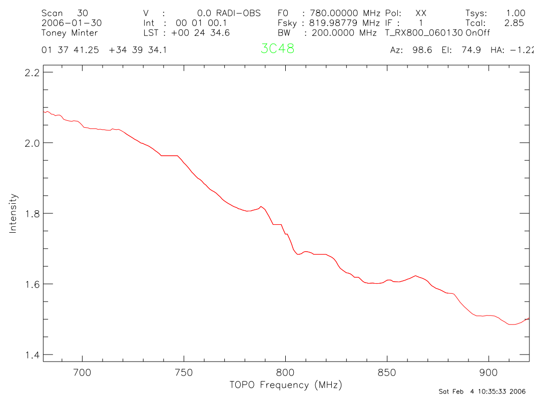

Figure 8: T_{cal} values for the Prime Focus 800 MHz receiver for the linear XX polarization.

were derived from this same data set. The data were then calibrated independently for each 1 MHz channel with the spectra using the method presented in § 2.1.3.

The result of calibrating this data using equation 45, which assumes an average value for the calibration noise diodes and the system temperature are shown in Figure 10 as the green data sets. The red lines in Figure 10 show the results when using a frequency dependent calibration.

From Figure 10, we first see that the average T_{cal} and T_{sys} calibration schemes produce an incorrect spectral index for the source. The reason for this is easily surmised when you compare Figure 10 with Figure 9 - the Galactic background radiation contributes significantly to the overall $T_{sys}(\nu)$. Furthermore, the Galactic background emission has a strong frequency dependence. Secondly, from Figure 10 we see that the average T_{cal} and T_{sys} calibration results in the two spectra not agreeing very well where there is overlap. This is not the case for the frequency dependent calibration.

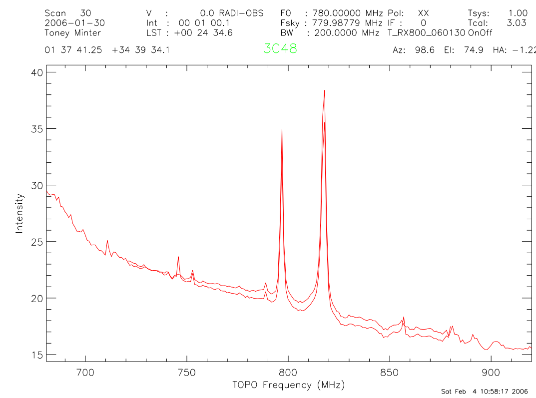

Figure 9: T_{sys} values for the Prime Focus 800 MHz receiver for the linear XX polarization. The data are from two different 200 MHz bandwidths shifted by 40 MHz. There are slight differences between the $T_{sys}(\nu)$ values at the same frequencies between the two bandwidths. These are possibly due to the different contributions of the IF signal path (amplifiers, etc.) to the T_{sys} values or from non-linear gains in the different IF paths. Note the two receiver resonances.

3 DC Offsets In GBT Backends

3.1 Spectrometer

The Spectrometer is an autocorrelation spectrometer (XF correlator) whose A/D is achieved either by 100 MHz samplers or by 1.6 GHz samplers. These samplers convert the analog signal into either a three level or nine level digital signal.

A simplistic description of how the 1.6 GHz, 3-level samplers work is as follows. The input signal is split into two exact copies, each with the same power level (or as close to it as possible). One copy of the signal is sent through a comparator to see if the signal's power level is above a high limit. The other copy goes to a comparator to see if the signal is below a low limit. The output of the two comparators is then used to determine which of the 3 levels that the digitized signal will occupy.

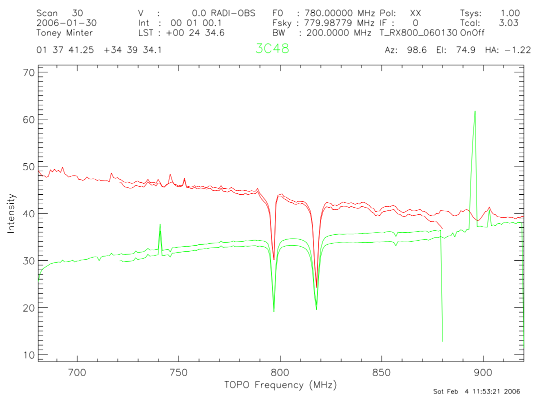

Figure 10: Red - calibrated data using frequency dependent values for $T_{sys}(\nu)$ and $T_{cal}(\nu)$. Green - calibrated data using equation 45. It is easily seen that the calibration using equation 45 produces an incorrect spectral index for this source. You can also see that the spectra between the two bandpasses do not agree where they overlap. However, they agree to a better extent when a frequency dependent calibration is used.

The high and low level thresholds for the comparators were set so that a nominally "balanced" input signal would produce the optimal statistics (i.e. Signal to Noise) for the samplers. However, the high and low level thresholds are known to vary (slightly) in time with the result that biases are introduced into the data. However, these detectors should not have any significant DC offsets. Furthermore, there is no simple method that could be used to measure any DC offset for the spectrometer (without significant cabling and test hardware required).

3.2 Spectral Processor

The Spectral Processor is an FX correlator. The A/D in the spectral processor is done with 32 level sampling (9 bits) in a similar fashion to that of the spectrometer. Like the spectrometer, the DC offset of the spectral processor cannot be easily measured.

3.3 DCR

The DCR digitizes data via Voltage-to-Frequency (V/F) conversion and then utilizing a frequency counter. The V/F nominally takes a 1 volt input signal and creates an approximate 1 MHz output. The frequency counter then converts the V/F output frequency to counts (i.e. the average frequency) during an integration time.

The V/F conversion is very susceptible to having DC offsets where a zero volt input will still create a output frequency. Furthermore, the V/F could posses a threshold below which it always outputs a zero frequency signal - effectively having a negative DC offset.

4 How to Measure the DCR DC Offsets

It is possible to make an approximate measure of the DCR DC offsets. This can be done by setting the IF Rack input to an unused input and routing the signal to the DCR directly from the IF Rack. The un-used input should be terminated for a better, absolute measurement of the DC offset. An unterminated input can give an order of magnitude value that is susceptible to jumps and variations as the impedance between the naked connector and the ambient medium changes due to temperature variations, etc.

5 DCR DC Offset Measurements

The data shown below was obtained on July 7, 2004 as part of the Prime Focus 800 MHz band receiver checkout. During the checkout I performed an OnOff observation of 3C 286. The off position was +60 arcminutes from 3C 286. The switching period was 0.2 seconds and data was take for 60 seconds on each position. Optical Drivers 1, 3, 6 and 7 were used and provided bandpass from 680 MHz to 920 MHz (the entire receiver bandpass) to the DCR. Optical Drivers 1 and 6 provided the X polarization signal to the DCR while Optical Drivers 3 and 7 provided the Y polarization. Two more scans were made with the same settings except that the IF Rack inputs where changed to ports that were "Unused" and terminated. This was done so that no signal was arriving at the DCR so that the DCR Zero Offsets could be measured.

In Figures 11 through 14 the raw data from the DCR for the DCR Zero Offsets measurements is shown. In each of the Figures 11–14 the signal on OD1 is red, OD3 is green, OD6 is blue and OD7 is magenta.

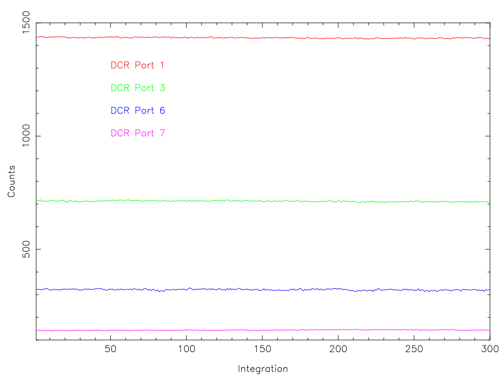

Figure 11: Cal signal, 3C 286, Zero Point measurement.

The DC offset terms are between 0.1–1.0% of the T_{sys} raw counts as determined from the off source scans.

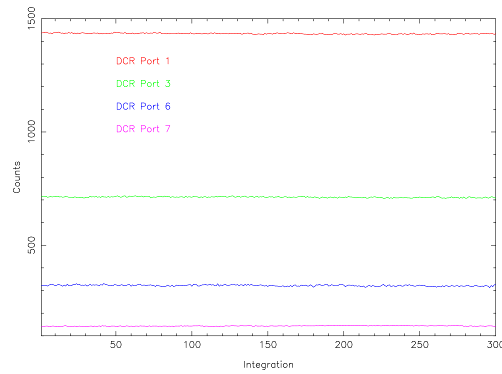

Figure 12: Cal signal, 3C 286, Zero Point measurement.

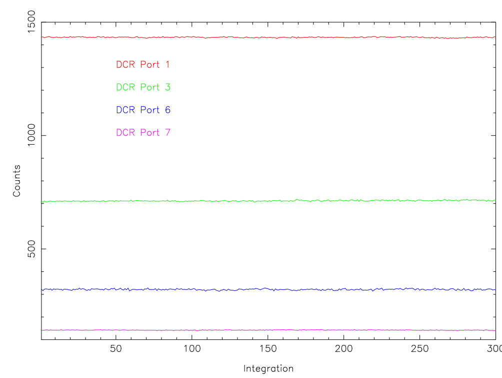

Figure 13: Cal signal, 3C 286, Zero Point measurement.

6 Conclusions

The following conclusions can be drawn:

1. Aips++/DISH (Nod only) and GBTIDL version 1.1 and earlier have incorrect calibration schemes.

2. Incorrect calibration can lead to apparent nonlinearities in the data that don't really exist.

3. Incorrect calibration can also create baseline structure.

4. With proper calibration the DC offset terms should not be a factor for spectral line observations.

5. Averaging over N noise diode on/off cycles will be necessary for correct calibration.

6. The gain for continuum observations must exclude data samples affected by point-like continuum sources.

7. For continuum mapping DC offset terms are not

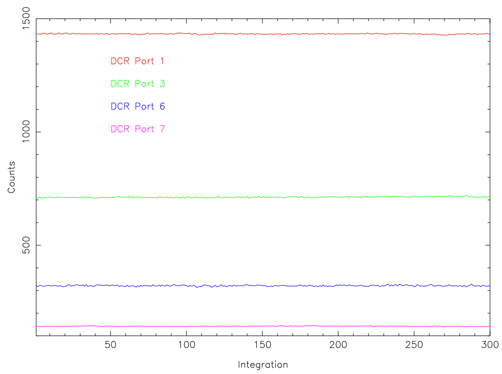

Figure 14: Cal signal, 3C 286, Zero Point measurement.

an issue if a constant background (i.e. a baseline) can be removed from the map.

8. For absolutely calibrated continuum data measurements of T_{sys} and the DC offset will have to be made.

9. The first 5 to 10 seconds of any scan must be flagged to remove the antenna not on source data.

10. The every 0.1 second antenna position measurements can be used in calibration to remove the affects of the antenna servo system.

11. A measurement of the feed-arm vibrations should also be included in the data sets so that their affects can be removed in the calibration.

12. Using a scalar value of T_{sys} and T_{cal} leads to incorrect fluxes after calibration.

13. The GBT data must use frequency dependent calibrations.